11

Real-Time Analysis to Evaluate Crystallization Processes

João F.Cajaiba da Silva, Andréia P. M. da Silva and Rodrigo C. de Sena
Instituto de Química – Universidade Federal do Rio de Janeiro
Brazil

1. Introduction

Crystallization is one of the most important unit operations employed by the pharmaceutical, microelectronics, food and fine chemicals industries for the production of solid products with high added value. This operation can be used as a method to perform separation and purification of crystalline compounds such as proteins, polymers, pharmaceuticals, inorganic salts, etc. (Févotte & Klein, 1995; Feng & Berglund, 2002; Mersmann, 2001; Lewiner et al., 2001; Mullin, 2001; Liotta & Sabesan, 2004; Joung et al., 2005; Pelberg et al., 2005; Derdour et al., 2011).

The experimental conditions used during a crystallization process may alter the physical properties of the final product such as its chemical purity, crystal size distribution and morphology. These properties can have impacts on the subsequent purification operations such as filtration, washing and drying, and can also alter the bioavailability of pharmaceuticals (Sabesan & Liotta, 2004). Polymorphism is another issue related to the crystallization process that has profound importance in the pharmaceutical industry because it can alter the kinetics of a crystal's solubilization and in some cases polymorphs present problems of toxicity (Fujiwara et al., 2005).

The challenges involved in controlling crystallization are significant, since the kinetic parameters of the process are strongly affected by several factors such as the presence of impurities (Gunawan et al., 2002; Ma et al., 1999; Rauls et al., 2000; Poddar, 2002), breaking of crystals (Kougoulos et al., 2005; Gahn & Mersmann, 1995) and clustering (Yu et al., 2005; Paulaime et al., 2003) among other effects that are difficult to characterize.

The identification and control of factors that affect the final quality of crystals are essential to ensure uniformity among different batches and to improve product quality. The development of more accurate and sensitive sensors for real-time analysis of crystallization must allow significant advances in monitoring, control and optimization of crystallization processes (Liotta & Sabesan, 2004).

The accuracy of off line methods for evaluating crystallization processes is strongly dependent on sampling. When the collected samples do not represent the whole, the errors introduced may cause a misinterpretation of the crystallization process. By using real-time analysis these types of errors can be greatly reduced. The possibility of performing in situ analysis of crystal size distribution, crystal shape, crystal habit, agglomeration and breakage

can indicate what changes should be made to the crystallization process parameters such as cooling and stirring rates and time for seeding. The optimization of these parameters allows crystals of the desired characteristics to be obtained (Yu et al., 2004).

This section is intended to give a brief overview of crystallization processes and the methods dedicated to monitor them in real-time. Additionally, a comparison between four in line methods to determine the onset of adipic acid crystallization was performed.

1.1 Solubility and supersaturation

The determination of the solubility of a solid in a specific solvent is a key step in the study of crystallization processes. The solubility curve is used as a benchmark to assess the degree of supersaturation and the metastable zone limits. The solubility or condition of saturation is determined experimentally by heating a suspension and observing the temperature at which the solid phase is completely dissolved. The cooling of a saturated solution results in a system that is not in thermodynamic equilibrium, a supersaturated solution (Mullin, 2001; Giulietti et al., 2001).

The supersaturation is the driving force for crystallization processes and can be defined as the difference between the chemical potential of a solute in a supersaturated solution and the chemical potential of the saturated solution. Supersaturation can be created by cooling, by adding an anti-solvent, by performing a chemical reaction that generates a product of lower solubility, by solvent evaporation, etc. Among the methods used to create supersaturation, cooling is the most used. The usage of this method is restricted to substances whose solubility changes significantly during a temperature variation. The expected properties of the solid material, as well as economic aspects, form the basis for making a decision about which method should be used to create supersaturation (Mullin, 2001; Giulietti et al., 2001).

The difference between the concentration of a compound in a supersaturated solution, c, and its concentration in a saturated solution, c*, is known as absolute supersaturation and is expressed by equation 1.

$$\Delta c = c - c^* \tag{1}$$

When Δc is greater than 0, the system is supersaturated. Another important parameter is the supersaturation ratio, S, which is defined by equation 2. In this case the system is said to be supersaturated when S is greater than 1.

$$S = \frac{c}{c^*} \tag{2}$$

1.2 Metastable zone width

Supersaturated solutions exhibit a metastable region, where despite the instability of the system, there is no separation of a solid phase. The determination of this region is, in general, the first phase in the design of a batch cooling crystallization process. The metastable zone width (MZW) is a property that depends on several characteristics of the system (cooling rate, solute concentration, stirring rate, thermal history of the solution, presence of impurities, etc.) (Liotta & Sabesan, 2004).

The metastable zone width is defined as the difference between saturation temperature and the temperature which is detected in the formation of the first crystals. This temperature difference is known as the maximum undercooling, ΔT_{max}. Figure 1 illustrates schematically the solubility curve and metastable zone boundary for a hypothetical case of a system cooled from an under saturated condition until the condition of supersaturation.

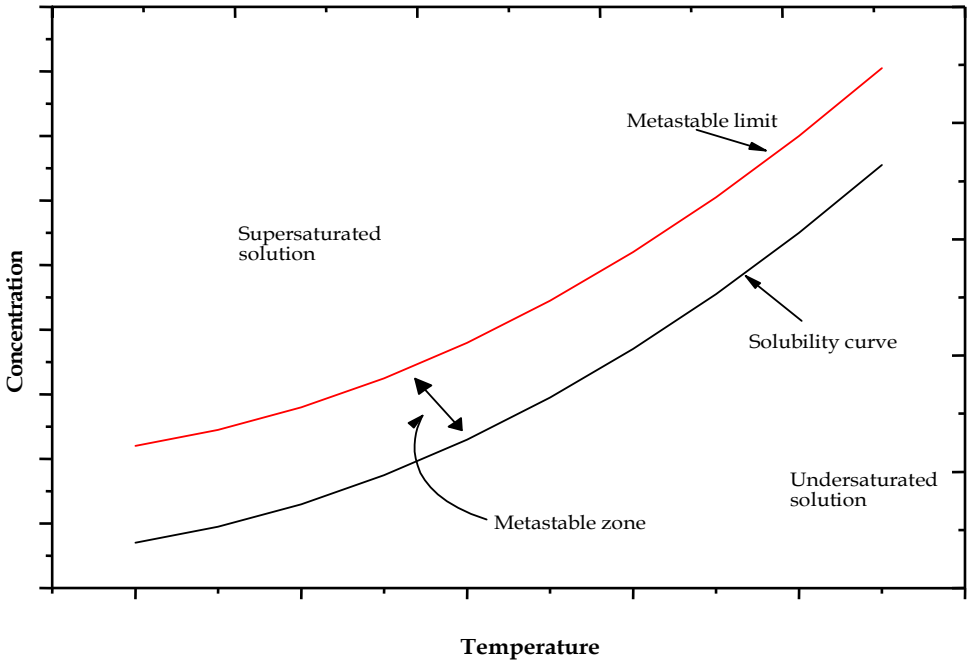

Fig. 1. Solubility curve and metastable zone.

In batch cooling crystallizations for example, maintaining the solution concentration profile within the metastable zone and close to the solubility curve promotes crystal growth and helps to avoid secondary nucleation (Beckmann, 2000). In the case of industrial crystallizers as a general rule, the level of supersaturation is maintained at about half the metastable zone (Marciniak, 2002).

1.3 Nucleation and crystal growth

The supersaturation is the main requirement for crystallization to occur and its creation does not imply the immediate separation of the phases. In a supersaturated solution, part of the dissolved solute tends to reorganize again to form the solid phase. However, the formation of the solid phase (positive energy) implies the generation of an interface (energetically unfavourable). Therefore, for the formation of nuclei to occur within the solution, it is necessary that this barrier is overcome (Mullin, 2001; Ulrich & Strega, 2002; Giulietti, 2001).

The nucleation rate depends on the supersaturation. When the supersaturation is extremely high, the nucleus formation is a random process and difficult to reproduce. For this reason, whenever possible, this condition is avoided in industrial applications (Mullin, 2001).

The crystal growth also depends on the supersaturation level. High growth rates lead to products with a degree of purity lower than those generated in conditions of lower supersaturation owing to the inclusion of liquids and other impurities. From the industrial point of view there is a compromise between the desired characteristics of the products and the economic efficiency of the process. This means that is not always possible to carry out crystallizations with a low rate of crystal growth because such a condition significantly increases the residence time of the product inside the crystallizer (Mullin, 2001; Ulrich & Strege, 2002).

1.4 Sensor technologies for monitoring crystallization processes

Continuous monitoring and control of crystallization processes in real-time require the use of sensors able to provide information regarding product quality and critical process variables.

The methods used to assess information of the products obtained from crystallization processes can be divided into four main groups (Yu et al., 2004):

- off line methods: the analysis is performed after sampling;
- on line methods: the sample stream is diverted from the crystallizer for analysis and subsequently returned to the system;
- in line methods: sensors are integrated into the crystallizer and provide real-time information about the process. The sensors are in direct contact with the material and can cause disturbances in the system;
- non-invasive methods: sensors are integrated into the crystallizer and provide real-time information of the process. In this case, the sensors do not come into direct contact with the material.

The real-time analyses described in this chapter can be included in the in line and the non-invasive methods.

1.4.1 Attenuated total reflectance Fourier transform infrared spectroscopy (ATR-FTIR)

ATR-FTIR is a consolidated technique in the monitoring of crystallization processes (Chen et al., 2009; Kadam et al., 2011; Pöllänen et al., 2006; Qu et al., 2009; Sheikhzadeh et al., 2008; Liotta & Sabesan, 2004). The method allows estimating the degree of supersaturation of the system by measuring the concentration of solute in the solution. The only prerequisite for application of the technique is the absorption of infrared radiation in the medium by the solute. The sensor used in this method has an element of internal reflection of high refractive index. The radiation passes through the element of reflection, being reflected when it encounters a material with lower refractive index. The amount of reflected radiation depends on the angle of incidence on the interface and when this angle is greater than a critical angle (depending on the ratio between the two refraction index) the refraction is attainable. However, radiation penetrates only a short distance into material of lower refractive index; this radiation is called the evanescent radiation (evanescent wave). Thus, if a sample is able to absorb infrared radiation, the beam is attenuated at frequencies absorbed by the sample (Man et al., 2010; Dunuwilaa et al., 1994).

1.4.2 Focused beam reflectance measurement (FBRM)

The FBRM measurement principle is based on backward light scattering. A laser beam is coupled to a probe via an optical fibre. This laser beam is deviated from the probe's central axis and focused into a disperse medium with an optical conduit. When this laser beam intersects with a particle, light scattering occurs. A certain fraction of the light is scattered back into the system. This back scattered light is coupled via a beam splitter to a second fibre and conduced to a detector. The rotational velocity of the laser is constant. The time span in which back scattering is detected is therefore directly proportional to the path length of the laser on the particle. It is assumed that the particle velocity is small compared to the laser rotational velocity. The length of the laser path on the particle is therefore proportional to the time span in which scattering is detected. This path length is called a chord length. Depending on the laser position, different chord lengths are measured even for a single particle. Those chord lengths are generally different from any characteristic particle length. In order to calculate the particle size distribution from the chord length distribution, a model is needed. This model has to cover all relevant aspects of the measurement technology (Kail et al., 2008; Barrett & Glennon, 2002). Figure 2 presents a schematic view of the Mettler Toledo FBRM probe.

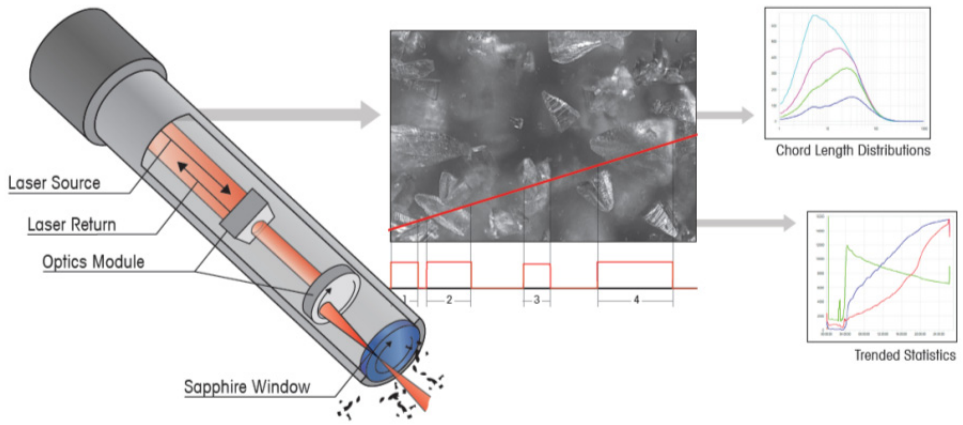

Fig. 2. Measurement principles of the Lasentec FBRM probe.

Just as with the ATR-FTIR technique, the FBRM is a well-established method of monitoring crystallization processes (Sun et al., 2010; Barrett & Glennon, 2002; Czapla et al., 2010; Sheikhzadeh et al., 2008; Nguyen & Kim, 2008).

1.4.3 Calorimetry

The principle of reaction calorimetry is based on the heat flow in processes involving changes in chemical or physical properties. The rate of release or absorption of heat is a parameter dependent on the kinetics and thermodynamics of the process under study (Gesthuisen et al., 2005; Mantel & Meyer, 2008). The combination of heat flow with the mass balance allows us to estimate the conversion of the instantaneous and cumulative process under study. Reaction calorimetry is non-invasive, fast, robust, relatively simple and its

principle is based on the measurement of temperature differences (Gesthuisen et al., 2005; Mantel & Meyer, 2008). From the industrial point of view, calorimetry is a technique of great importance because it allows safely scaling up a process from pilot to industrial scale (Gesthuisen et al., 2005). The method finds application in the study of polymerization reactions (Benamor et al., 2002; Elizalde et al., 2005), biotechnological processes (Marison et al., 1985), study of supercritical fluids (Lavanchy et al., 2004; Mantel & Meyer, 2008), optimization of chemical reactions (Barton et al., 2003) and determination of kinetic parameters of chemical reactions (Silva et al., 2003; Seiceira et al., 2005) among other applications. There are few articles where heat flow calorimetry is applied to the study of crystallization processes (Févotte & Klein, 1995)

1.4.4 Image analysis

The use of Complementary Metal Oxide Semiconductor (CMOS) and Charge Coupled Device (CCD) cameras has been widely introduced in analytical chemistry for different reasons such as fast image capturing, stable background and good linearity (Jolling et al., 2007). These sensors are capable of converting the intensity of light that focuses on it in digital storable values as bits. The analytical response that generates an image representing the patterns of the colours Red (R), Green (G) and Blue (B). These patterns are known as RGB 8 bits for each channel, totalling 256 levels. The combination of the three matrices (R, G and B) allows the acquisition of 16 million colours (Gaiao et al., 2006; Safavi et al., 2007). Different methodologies employing this image analysis has been described in literature. A digital camera was used as a sensor for simultaneous determination of Al(III) and Fe(III) in alloys using the chrome azurol S(CAS) as chromogenic reagent (Maleki et al., 2004). An instrumental detection technique for titration based on digital images was proposed (Gaiao et al., 2006). A similar method for the measurement of lithium, calcium and sodium through the radiation emitted by the sample into an air-butane flame was developed (Lyra et al. (2009). Image analysis was also used for a real-time assessment of the coffee roasting process (Hernández et al., 2008). An approach employing a CCD camera as a sensor for recognizing volatile alcohols was described (Shirshov et al., 2007). A method based on external bulk video imaging was proposed for metastable zone identification in food and pharmaceutical crystallization processes, and showed good performance when compared to FBRM and ultra-violet visible spectroscopy (Simon et al., 2009). Additionally, CCD cameras have been used as detectors in clinical analysis and showed high detection sensitivity (Liang et al., 2004; Alexandre et al., 2001). The rapid improvements in digital camera technology provide the opportunity for the development of new methodologies employing digital cameras as an analytical sensor with high sensitivity, robustness, speed and low cost for implementation that reduces the analysis time.

2. Experimental part

In this section batch cooling crystallization of adipic acid will be used as a model to demonstrate the use of in line and non-invasive techniques for monitoring crystallization. For this purpose, four analytical tools with different physical principles were used. The procedures and techniques used in the experiments are described in the following subsections.

2.1 Materials and methods

2.2.1 Solubility

The solubility of adipic acid (99.8%) in ethanol (analytical grade) was determined for twelve different temperatures ranging from 16.0 to 64.0˚C. The experiments were performed in a 1.8-L Hastelloy jacketed reactor vessel connected to an RC1e reaction calorimeter. The solutions were prepared by successive additions of adipic acid to a solution containing ethanol at a stirring rate of 300 rpm. For measurements at 44.0˚C, the mass of ethanol used was 524.0g. The used mass for other temperatures are presented in Table 1. The solubilization temperature was maintained constant during the whole process.

Temperature (K)	Temperature (ºC)	Ethanol mass (g)
289.15	16.0	590.3
293.95	20.8	582.7
298.15	25.0	574.7
303.95	30.8	564.3
306.15	33.0	556.3
308.25	35.1	550.8
312.15	39.0	537.0
317.15	44.0	524.0
323.15	50.0	492.4
330,15	57.0	459.5
334.15	61.0	428.1
337.15	64.0	405.3

Table 1. Experimental conditions for testing the solubility of the adipic acid in ethanol.

The ATR-FTIR measurements were performed by using a Mettler-Toledo ReactIR IC10 spectrometer. The base unit contains the Fourier transform mid-infrared source and the mercuric cadmium telluride (MCT) detector that should be cooled with liquid nitrogen. The sample interface module (SIM) is the interface on the instrument base unit where the K6 (16 mm diameter) conduit connects. It contains the optics that transfer the infrared source light from the base unit to the probe in contact with the chemical materials contained in the vessel and then back to the detector. Measurements are taken optically using a diamond sensing element that uses a multiple reflection ATR crystal and a gold seal between the metal housing and the sensor. Figure 3 illustrates schematically the K6 Mettler Toledo probe tip.

The focused beam reflectance measurements were obtained by using a Mettler-Toledo Lasentec D600L probe consisting of a Hastelloy C-22 tube with the sensor at one end with an optical diameter of 19 mm and a length of ~406 mm. The FBRM laser provides a continuous beam of monochromatic light with a wavelength of 780 nm. The beam is located approximately 3 mm to the focal point.

The ATR-FTIR and FBRM probes were kept immersed in the adipic acid solution 5 cm above the propeller stirrer. Infrared spectra obtained from 4000 to 650 cm^{-1} at 4 wave numbers resolution were collected at 15 s intervals with each spectrum averaged over 30 scans.

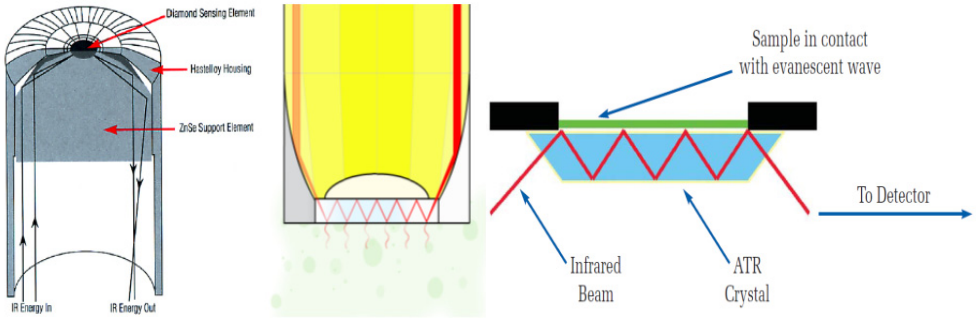

Fig. 3. Schematic draw of the Mettler Toledo K6 probe tip.

2.2.2 Batch cooling crystallization

The batch cooling crystallization experiments were carried out in a double walled glass reactor with a capacity of 2.0L. The solutions were stirred by a propeller stirrer at 300 rpm. The experimental setup is schematically presented in Figure 4.

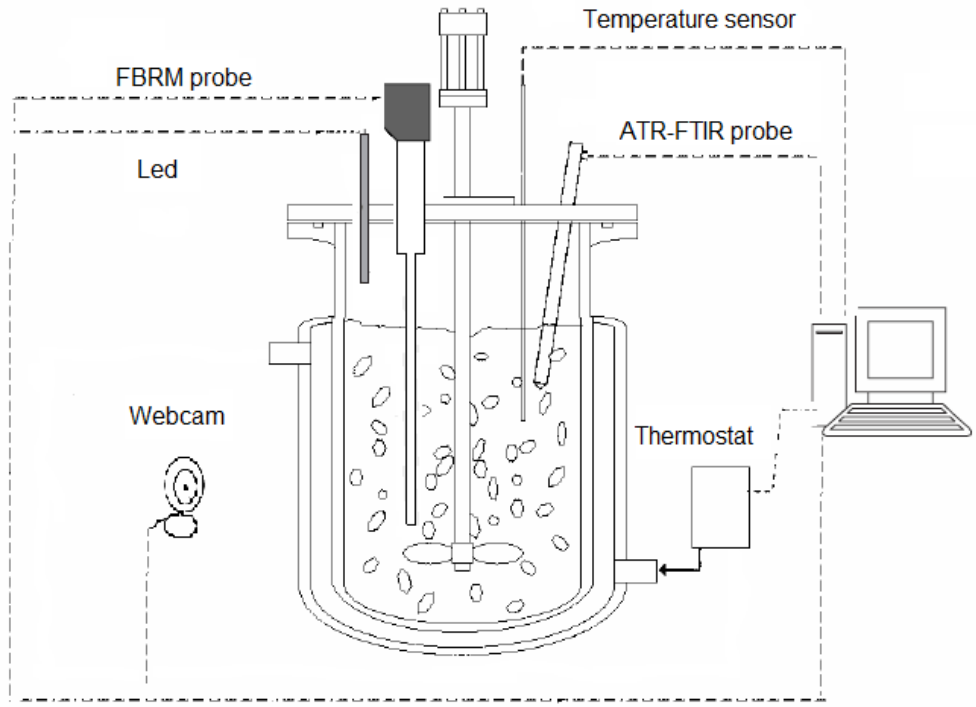

Fig. 4. Experimental setup.

The mass of ethanol used in each run was 600 g and the amount of adipic acid was varied from 91.2 to 279.9 g. The temperature was controlled by the precise RC1e thermostat. The

temperature of solution was kept 5°C higher than that saturation condition in order to assure that no crystal was presented in the solution prior to starting the cooling process. After 0.5 h, the solution was cooled at constant rate of 0.2 and 1°C/min, until the onset of crystallization. The experimental conditions of experiments are presented in Table 2.

Concentration (mass %)	Temperature at the start of cooling (°C)	Final temperature (°C)	Mass of adipic acid (g)
13.2	30.0	-2.00	91.20
15.1	35.0	5.00	106.8
17.3	40.0	10.0	125.2
19.7	45.0	15.0	146.8
22.3	50.0	15.0	172.2
25.2	55.0	20.0	202.1
28.4	60.0	25.0	237.6
31.8	65.0	25.0	279.7

Table 2. Experimental conditions for crystallization experiments of adipic acid in ethanol.

In situ methods, FBRM and ATR-FTIR, were used to monitor adipic acid crystallization. Non-invasive measurements were carried out by monitoring the heat released and the image patterns of colours red, green and blue during the crystallization. Images of experiments were acquired by using a low cost PC webcam (Microsoft Life Cam VX-2000). The webcam was placed externally and, in order to avoid interferences by external light and to maintain the CCD noise under controlled conditions, the reactor was enclosed with a black box. The images were captured during whole experiments. A light-emitting diode (LED) was used as a source of illumination. The images acquired were analysed according to their patterns of colour red, green and blue, and for this purpose software was developed which allows the evaluation of alteration in these patterns of colours. The software enables the analysis of the whole image or the user can define a specific region previously selected from an image. The software automatically saves the coordinates of the delimited region for all digital images and calculates the R, G and B values averaging all pixels.

The heat released during the crystallization was monitored using the RC1e. To be able to calculate the heat flow during the crystallization, the total heat transfer coefficient (U) and the heat capacity (Cp) of the solution of adipic acid were measured.

3. Results and discussion

This section presents the results obtained in the study of solubilization of adipic acid in ethanol as well as its crystallization, evaluating the possibility of using calorimetry, infrared (ATR-FTIR) and FBRM as techniques for determining the width of the metastable zone.

3.1 Determination of the solubility of adipic acid

The solubility curve of adipic acid in ethanol, presented in Figure 5, was prepared according to procedure in literature that used ATR-FTIR and heat flow to calculate the solubility curve of adipic acid in acetone (Silva & Silva, 2011).

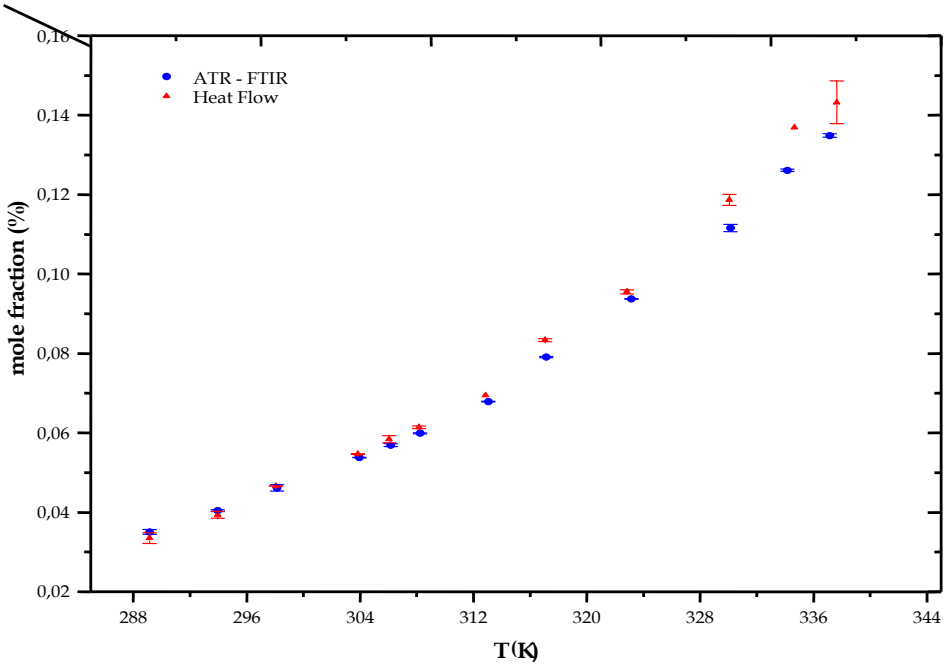

Fig. 5. Solubility curves of adipic acid in ethanol by using ATR-FTIR and heat flow calorimetry.

3.2 Determination of the onset temperature for the crystallization of adipic acid in ethanol by heat flow calorimetry

Since during crystallization there is a decrease in entropy, the second term of the Gibbs free energy (equation 3) becomes positive and therefore, for ΔG to be negative, it is necessary that the change in enthalpy is negative, which shows that the crystallization processes are exothermic.

$$\Delta G = \Delta H - T\Delta S \tag{3}$$

The heat flow for cooling at 1^0C/min is presented in Figure 6.

The analysis of Figure 6 shows that when the solution temperature was approximately 37.2°C, the jacket temperature was reduced by about 10°C, so that the cooling rate of 1°C/min could be maintained, meaning that an exothermic process had started. The heat flow measurement had a fast increase at the same moment indicating that the crystallization of the adipic acid (the exothermic process) had begun. In the initial moments of the crystallization there was an intense release of heat and soon after that the

release decreased and became nearly constant. The region where heat release is constant may be associated with the growth of crystals (Riesen, 2005). The heat release continued until the moment when the reactor temperature was maintained at 15.0 °C. With the constant temperature the heat flow remained stable, indicating that the process that was responsible for the release of heat had ceased. As the only process that was taking place inside the reactor was the crystallization of adipic acid, this release is solely related to this process.

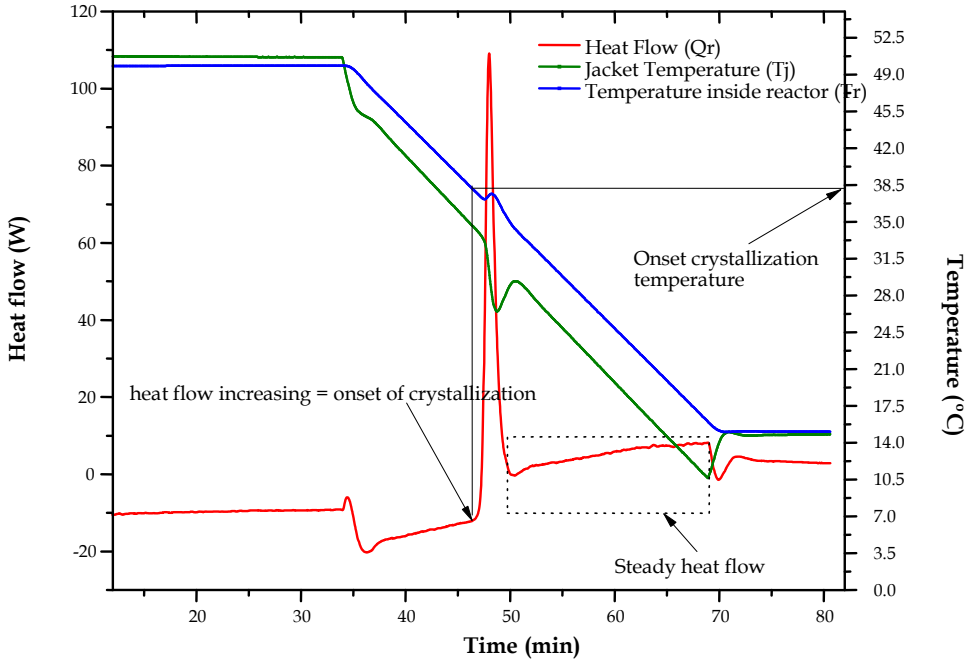

Fig. 6. Heat release curve (Qr), the temperature inside the reactor (Tr) and temperature of the jacket (Tj), obtained from crystallization experiments using an ethanol solution with initial concentration of 22%, cooled at a rate of 1°C/min and with a stirring rate of 300 rpm.

The maximum supersaturation achieved in the solution is a function of the maximum cooling achieved by the system. Thus, it is expected that the higher the maximum cooling achieved by a system, the greater the value of supersaturation in the medium. In general the smaller nucleation rates are obtained at lower cooling rates (Mullin, 2001). In order to check this information, the crystallization of adipic acid was performed at a lower cooling rate as presented in Figure 7.

The rate at which heat is released when employing a cooling rate of 1°C/min is higher than when using a cooling rate of 0.2°C/min.

The comparison between the results presented in Figures 6 and 7 confirms that the maximum heat released is a function of cooling rate.

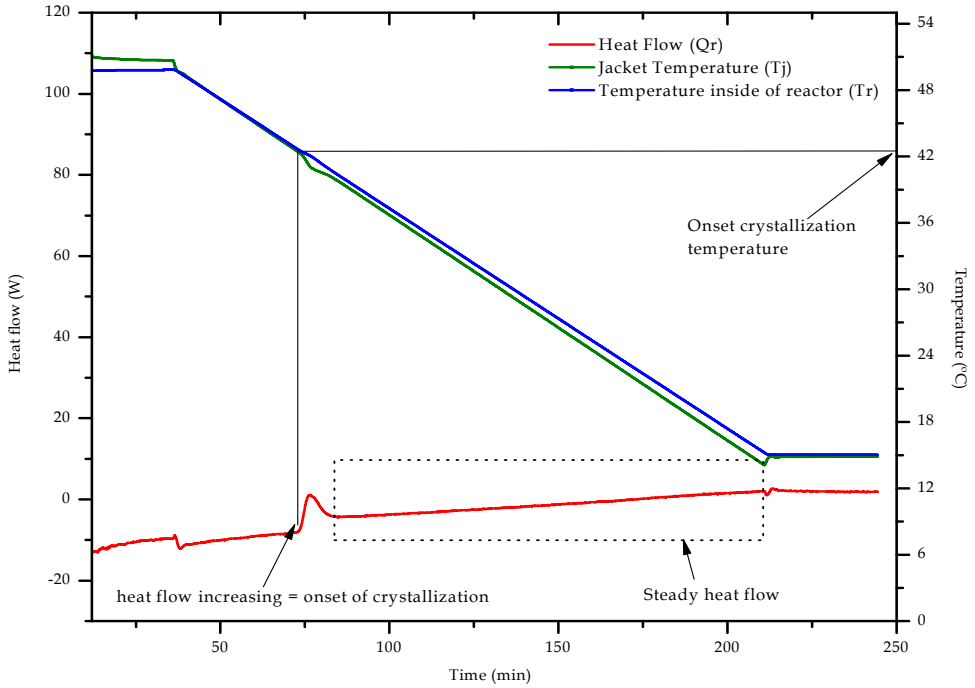

Fig. 7. Heat release curve (Qr), the temperature inside the reactor (Tr) and temperature of the jacket (Tj), obtained from crystallization experiments using an ethanol solution with initial concentration of 22%, cooled at a rate of 0.2°C/min and with a stirring rate of 300 rpm.

3.3 Determination of the onset temperature for the crystallization of adipic acid in ethanol by RGB image analysis

The image video analysis was performed by using software named MasterView RGB that captures images in real-time from a PC webcam by evaluating changes in the component's RGB colour pixel by pixel. The software automatically saves the coordinates of the delimited region for all digital images and calculates the RGB values averaging all pixels (de Sena et al., 2011).

Figure 8 shows the graphic interface of MasterView RGB for an adipic acid solution and Figure 9 presents the crystallization onset by measuring the RGB variation.

The method of image analysis is based on comparison of images. This procedure is comparable to human visual inspection and the method of image analysis has greater sensitivity and is not subject to misinterpretation.

The variation of the red channel during the crystallization of adipic acid is presented in Figure 10.

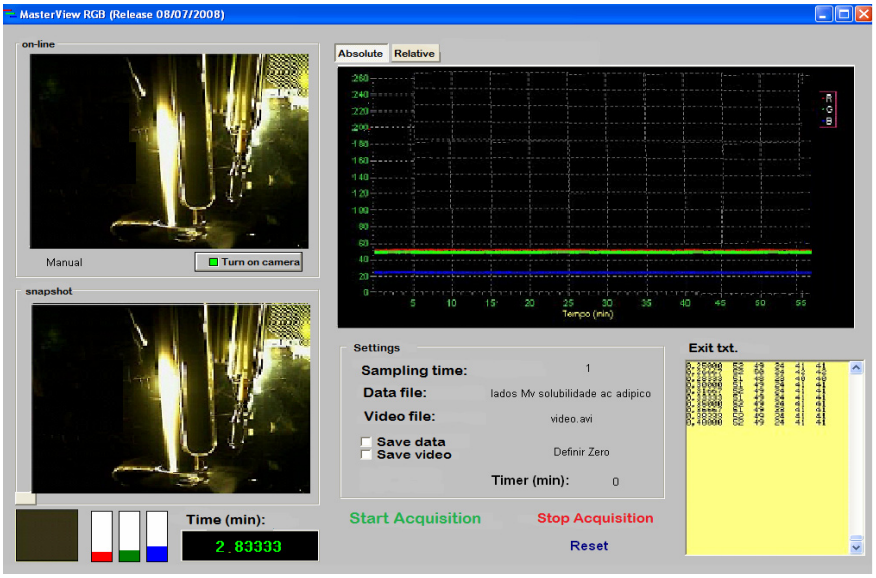

Fig. 8. Monitoring of the onset of the crystallization of adipic acid using the image analysis method (saturated solution).

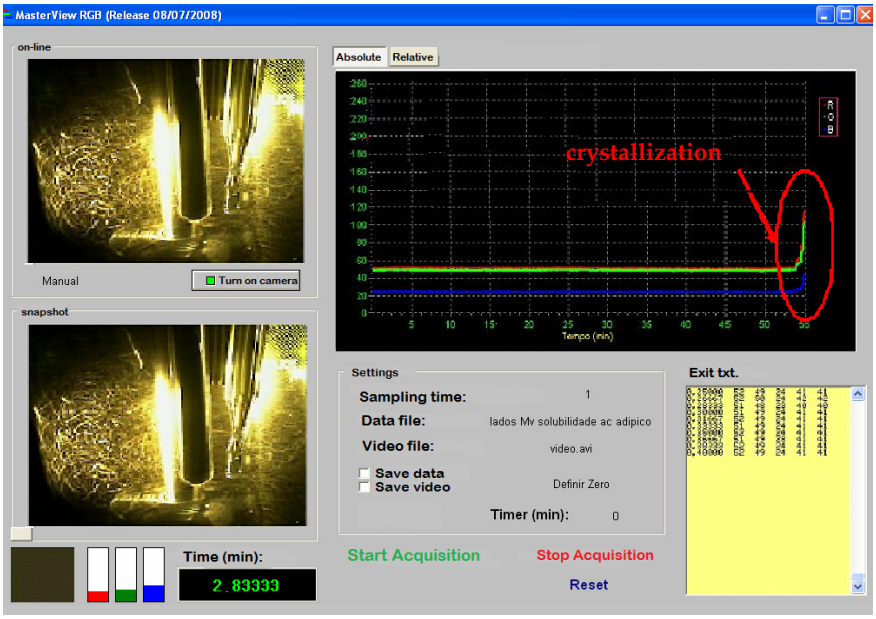

Fig. 9. Monitoring of the onset of the crystallization of adipic acid using the image analysis method (increasing the mass of adipic acid crystals due to cooling).

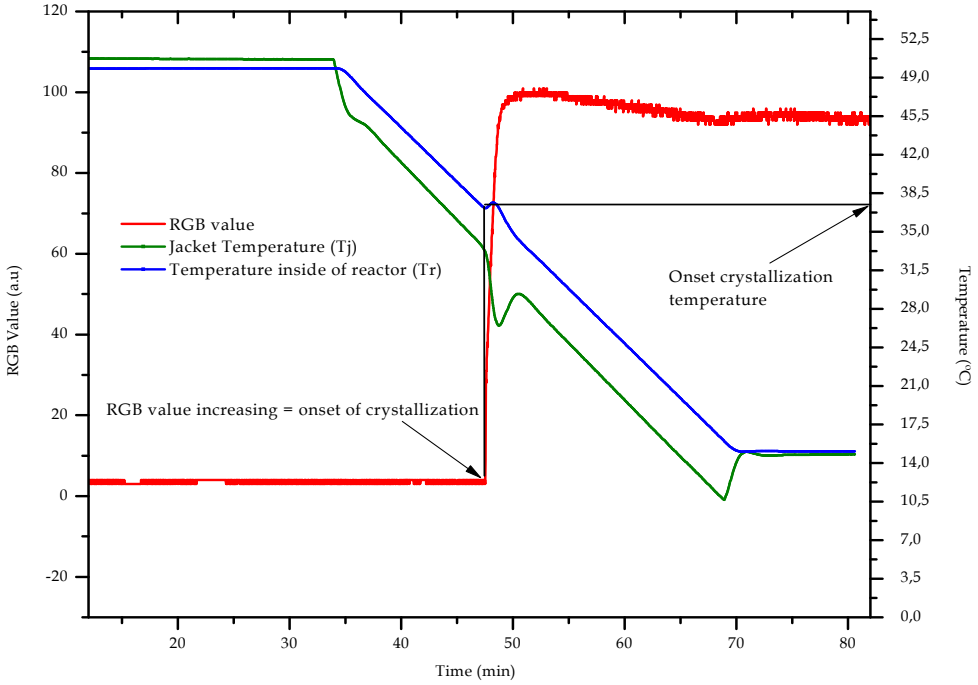

Fig. 10. Image analysis red channel, the temperature inside the reactor (Tr) and temperature of the jacket (Tj), obtained from crystallization experiments using ethanol solution with initial concentration of 22%, cooled at a rate of 1°C/min and with a stirring rate of 300 rpm.

As can be seen in Figure 8, before the crystallization of adipic acid (red signal channel close to zero), the red value increases immediately when the adipic acid crystallization starts. This result is in total accordance with the results obtained by heat flow calorimetry. It was established that the onset temperature of crystallization, determined by the variation in RGB signal, would be that corresponding to the time when the RGB signal began to increase.

3.4 Determination of the onset temperature of crystallization using infrared (ATR-FTIR)

The infrared absorption spectrum of adipic acid is presented in Figure 11.

The carbonyl stretching absorption region of carboxylic acids used in the ATR-FTIR analysis is indicated in Figure 11.

The analysis of crystallization of a solution of adipic acid in ethanol was accompanied by infrared (ATR-FTIR), through the decrease of the signal of the peak area for the absorption of carbonyl (C=O) in the medium. Figure 12 presents the carbonyl absorption variation during a crystallization process that started at 50 °C.

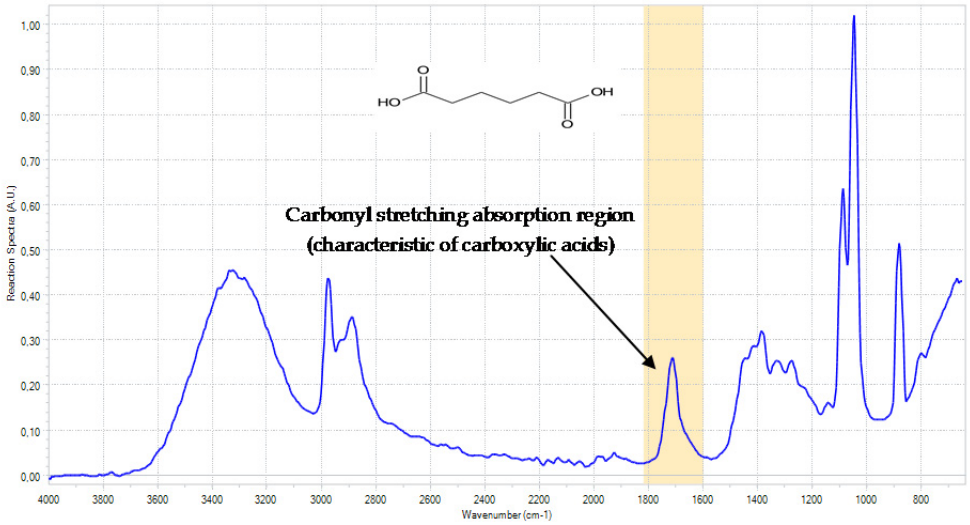

Fig. 11. ATR/FTIR spectra of adipic acid in the infrared region.

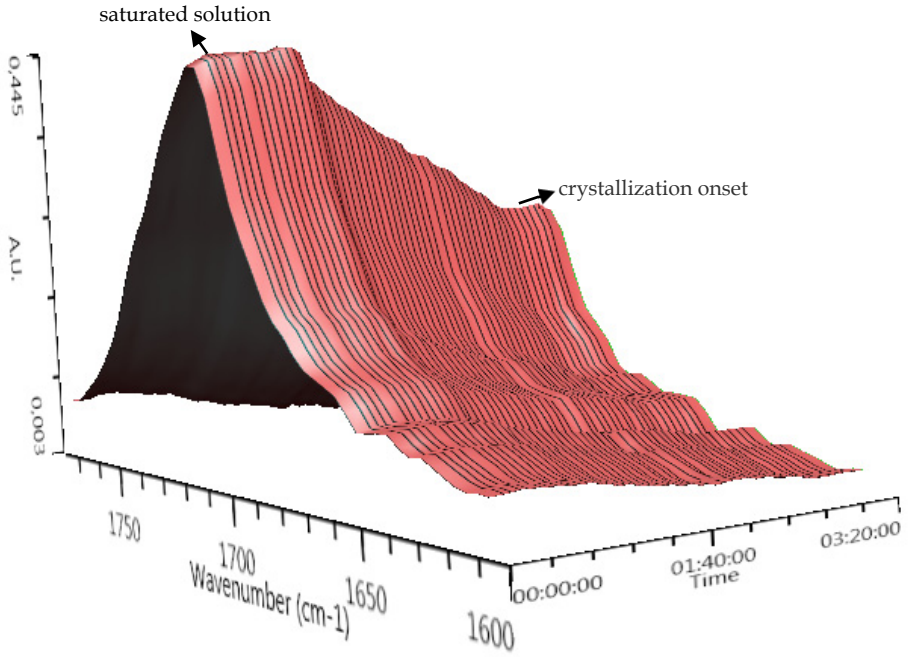

Fig. 12. Adipic acid carbonyl absorption variation measured in the interval of 1750-1600 cm^{-1}.

The carbonyl absorption trend related to the data presented in Figure 12 is presented in Figure 13.

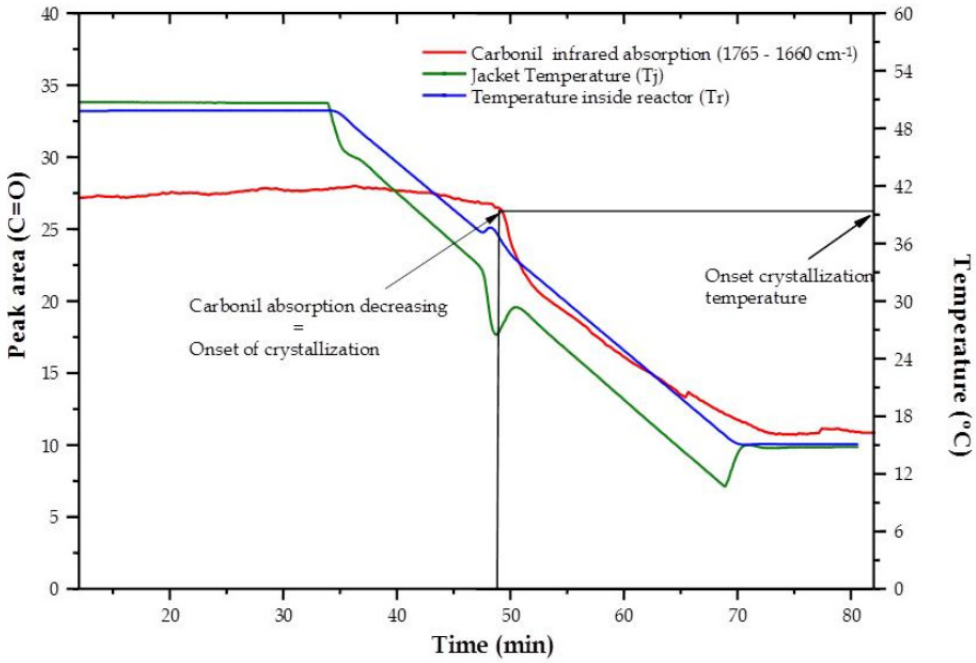

Fig. 13. Absorption curve of the carbonyl C=O (1765-1660 cm 1) in ethanol, the temperature inside the reactor (Tr) and jacket temperature (Tj), obtained from crystallization experiments using an ethanol solution with initial concentration of 22% , cooled at a rate of 1°C/min and stirring rate of 300 rpm.

The carbonyl absorption area presented a decrease at the precise moment the crystallization started. This observation is in total agreement with the fact that the ATR probe detects the concentration of adipic acid soluble in ethanol. A comparison between the infrared absorption for the cooling rates of 1 and 0.2^0C/min is presented in Figure 14.

The FTIR analysis may be considered as an indirect measurement of the kinetics of crystallization, since the ATR probe cannot detect the crystallized adipic acid. As expected, the diminution of the carbonyl absorption was more pronounced when the higher cooling rate was used.

3.5 Determination of onset temperature of the crystallization using Focused Beam Reflectance Measurement

The variation in the total chord counts obtained from the FBRM analysis can detect the crystallization onset. This signal remained in the form of a stable baseline, with a few counts per second before the formation of crystals. By the time the crystallization of adipic acid had started the chord counts increased dramatically. This behaviour can be seen in Figure 15.

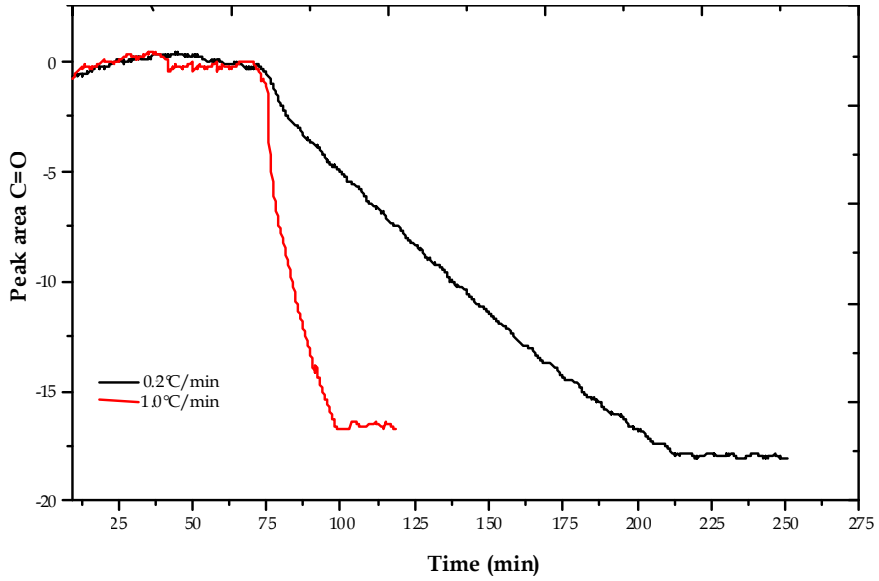

Fig. 14. Infrared absorption curve of the carbonyl C=O (1765-1660 cm^{-1}) of adipic acid during crystallizations performed at cooling rates of 1.0 and 0.2^{0}C/min.

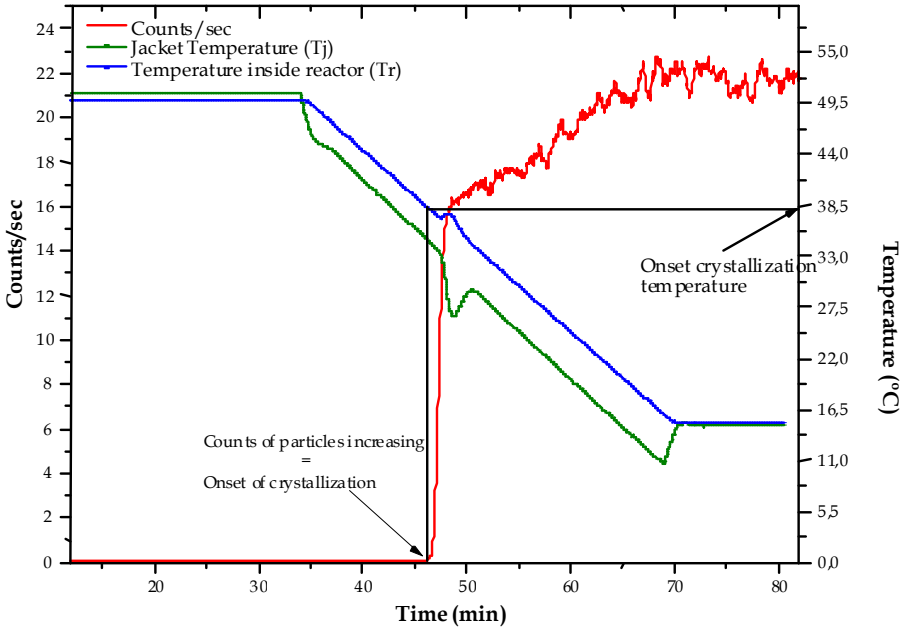

Fig. 15. Total chord counts (FBRM), the temperature inside the reactor (Tr) and temperature of the jacket (Tj), obtained from the crystallization experiments using a solution of ethanol with initial concentration of 22%, cooled at a rate of 1°C/min and stirring rate of 300 rpm.

The comparison between the chord length distribution in the crystallization onset with the values obtained in the end cooling, presented in Figure 16, can furnish information about crystal growth and this variation can also be detected by analysing the particle video microscopy images correspondent to these different moments that are shown in Figure 17.

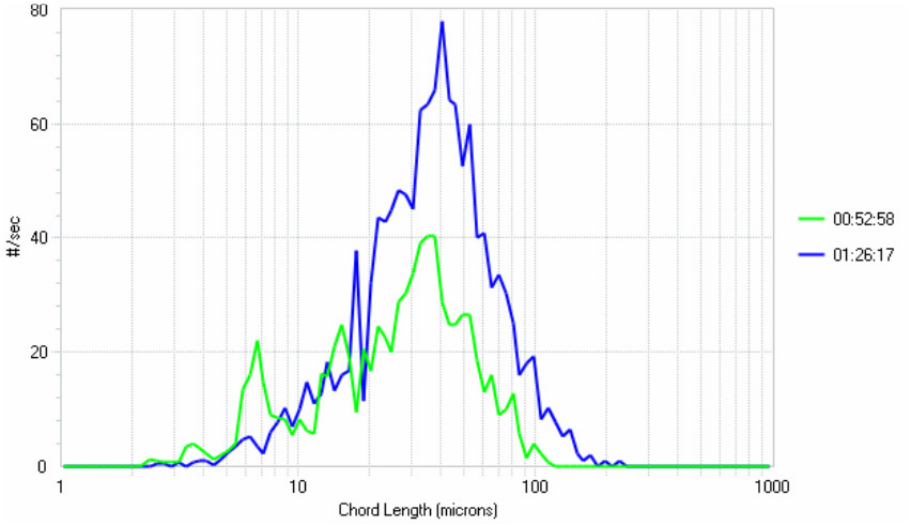

Fig. 16. Chord length distribution obtained in the crystallization onset, green curve and at the end of the experiment.

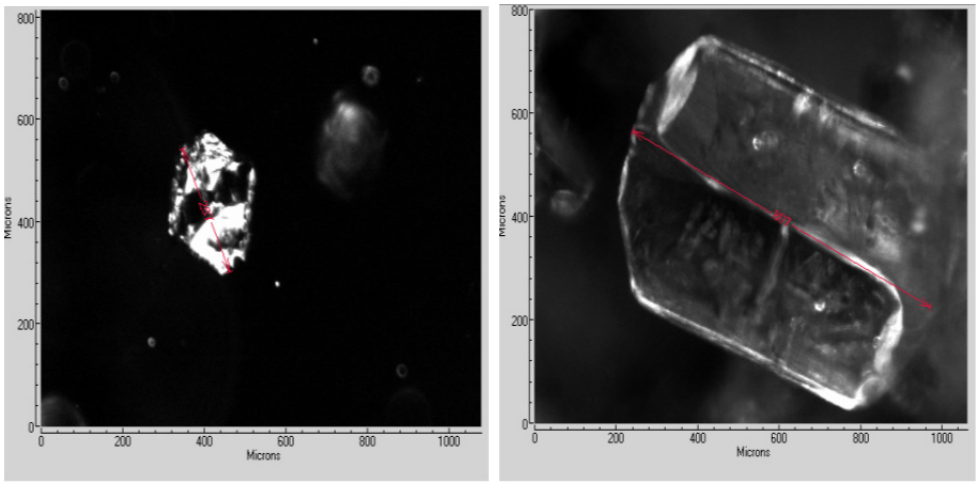

Fig. 17. Real-time particle video microscopy obtained in the crystallization onset (a) and in the end of the experiment (b).

The distributions shown in Figure 16 were displayed on a logarithmic scale on the horizontal axis (length of chords) for easy viewing. The shift to the right side in the chord

length distribution indicates crystal growth. The crystal sizes presented in Figure 17 confirm the crystal growth.

The average size of the chord length of adipic acid particles produced in the set of experiments is presented in Table 3.

concentration (% mass)	cooling rate (°C/min)	average size (μm)
13.2	0.2	75.20
13.2	1.0	65.24
15.1	0.2	76.91
15.1	1.0	73.11
17.3	0.2	84.36
17.3	1.0	73.59
19.7	0.2	73.48
19.7	1.0	70.76
22.3	0.2	119.4
22.3	1.0	77.47
25.2	0.2	106.7
25.2	1.0	88.88
28.4	0.2	127.9
28.4	1.0	80.31
31.8	0.2	132.2
31.8	1.0	88.78

Table 3. Average size of the chord length of adipic acid crystals in the different experimental conditions.

The results presented in Table 3 show that the average size of adipic acid crystals increases as the cooling rate decreases. This fact is directly correlated with the metastable zone width, which is directly proportional to the rate of nucleation (Nyvlt et al., 2001). Thus, the largest crystals were observed when the cooling rate was 0.2°C/min, the rate at which the narrowest metastable zone was maintained.

3.6 Determination of metastable zone width of adipic acid in ethanol

The metastable zone width of a system is dependent on the methodology employed for its determination. Depending on the sensitivity of the technique used to detect the onset of crystallization, significant deviations can occur between two different methodologies (Marciniak, 2002). For a satisfactory evaluation of the metastable zone limit, it is necessary that the reactor be cooled at a constant rate. This constant cooling can be seen through the linear behaviour of both the crystallizer temperature and the jacket of the reactor.

The onset crystallization temperatures determined by the different real-time methods are presented in Table 4 and the agreement between these data can be seen in Figure 18.

Adipic acid concentration (%)	T calorimetry (°C)	T infrared (°C)	T FBRM (°C)
13.2	16.45	16.13	16.23
15.1	18.02	17.78	17.90
17.3	24.44	24.34	24.20
19.7	30.91	30.70	30.79
22.3	37.34	37.16	37.28
25.2	42.77	42.70	42.72
28.4	50.30	50.24	50.27
31.8	57.22	57.11	57.19

Table 4. Comparison of the calorimetric method, infrared and total chord counts for the determination of the onset temperature of crystallization of adipic acid in ethanol using a cooling rate of 1°C/min.

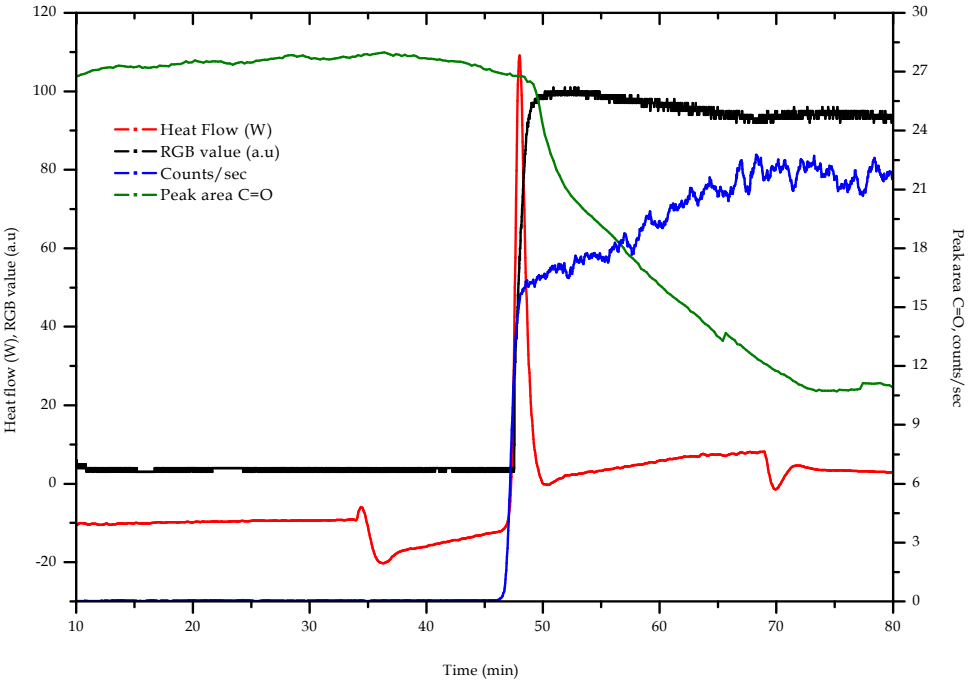

Fig. 18. Curves of the peak area of absorption of carbonyl (C=O), total count (FBRM), image analysis by RGB (**RGB**), calorimetry (heat flow) obtained from the cooling of a solution of 22% adipic acid in ethanol, cooled to 1.0 ° C / min with a stirring rate of 300 rpm.

The results presented in Figure 18, obtained by the different real-time analyses, were similar. In this case, the heat flow measurement presented higher sensibility than the other real-time analyses, but all techniques can be considered equivalent.

3.7 Study of the effect of the cooling rate on the metastable zone width of adipic acid in ethanol

Considering that the calorimetric method presented the highest sensibility, this was the chosen method to present the metastable zone limits for the crystallization of adipic acid by using cooling rates of 1.0 and 0.2^{0}C/min as presented in Figure 19.

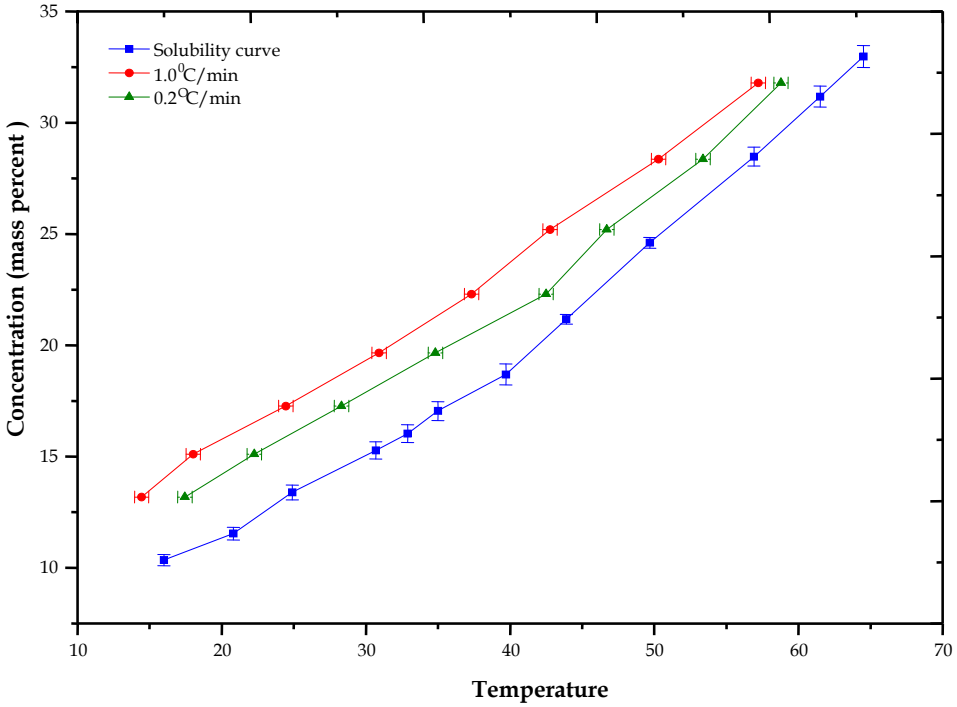

Fig. 19. Solubility curve of adipic acid in ethanol and the metastable zone limits determined at 1.0 and 0.2^{0}C/min.

The metastable zone width, expressed in terms of maximum cooling achieved, Δt, which is the difference between the saturation temperature, T saturation, and the onset temperature of crystallization, is reduced when the cooling rate is diminished. This statement can be confirmed by the data presented in Figure 19.

4. Conclusion

Considering that the experimental conditions employed during crystallization may affect physical properties of the product, such as its chemical purity, crystal size distribution and polymorphism and that these properties are completely related to the metastable zone width, accurate measurement techniques capable of providing data to construct solubility curves, as well as the onset of crystallization, are of vital importance. Off line analytical methods used to determine solubility curves and to detect the onset of crystallization present much higher errors than those that use real-time analysis for the same purpose. The

four real-time analyses used in this work, even though working in different ways, presented equivalent performance, indicating that all of them can be used as process analytical tools to evaluate crystallization processes.

5. References

Alexandre, I.; Hamels, S.; Dufour, S.; Collet, J.; Zammatteo, N.; De Longueville, F.; Gala, JL. & Remacle, J. (2001). Colorimetric Silver Detection of DNA Microarrays. *Analytical Biochemistry,* Vol.295, No.1, (August 2001), pp. 1-8, ISSN 0003-2697

Barton, B.; Gouws, S.; Shaefer, MC. & Zeelie, B. (2003). Evaluation and optimization of the reagent addition sequence during the synthesis of Atrazine (6-chloro-N^2-ethyl-N^4-isopropyl-1,3,5-triazine-2,4-diamine) using reaction calorimetry. *Organic Process Research and Development,* Vol.7, No.6, pp. 1071-1076, ISSN 1083-6160.

Barrett, P. & Glennon, B. (2002). Characterizing the Metastable Zone Width and Solubility Curve Using Lasentec FBRM and PVM Original. *Chemical Engineering Research and Design*, Vol.80, No.7, (October 2002), pp. 799-805 ISSN 0263-8762

Beckmann, W. (2000). Seeding the desired polymorph: Background, possibilities, limitations, and case studies. *Organic Process Research and Development*, Vol.4, No.5, (September 2000), pp. 372-383, ISSN 1083-6160

BenAmor, S.; Colombié, D. & McKenna, T (2002) On line calorimetry: Applications to the monitoring of emulsion polymerization without samples or models of the heat-transfer coefficient. *Industrial and Engineering Chemistry Research*, (May 2002), Vol.41, No.17, pp. 4233-4241, ISSN 0888-5885.

Chen, ZP.; Morris, J.; Borissova, A.; Khan, S.; Mahmud, T.; Penchev, R. & Roberts, KJ. (2009). On-line monitoring of batch cooling crystallization of organic compounds using ATR-FTIR spectroscopy coupled with an advanced calibration method. *Chemometrics and Intelligent Laboratory Systems*, Vol.96, No.1, (March 2009), pp. 49-58, ISSN 0169-7439.

Czapla, F.; Kail, N.; Öncül, A.; Lorenz, H.; Briesen, H. & Seidel-Morgenstern, A. (2010). Application of a recent FBRM-probe model to quantify preferential crystallization of dl-threonine. *Chemical Engineering Research and Design*, Vol.88, No.11, (November 2010), pp. 1494-1504, ISSN 0263-8762

Derdour, L.; Pack, S. K.; Skliar, D.; Lai, C. J. & Kiang, S. (2011). Crystallization from solutions containing multiple conformers: A new modeling approach for solubility and supersaturation. *Chemical Engineering Science*, Vol.66, No.1, (January 2011) pp. 88-102, ISSN 0009-2509.

Dunuwila, D. D.; Carroll II, L. B.; Berglund, K.A. (1994). An investigation of the applicability of attenuated total reflection infrared spectroscopy for measurement of solubility and supersaturation of aqueous citric acid solutions. *Journal of Crystal Growth*, Vol.137 Nos.3-4 (April 1994) pp. 561-568 ISSN 0022-0248

Elizalde, O.; Azpeitia, M.; Reis, M. M.; Asua, J. M.; & Leiza, J. R. (2005). Monitoring emulsion polymerization reactors: Calorimetry versus Raman spectroscopy. *Industrial and Engineering Chemistry Research,* Vol.44 No.18 (July 2005) pp. 7200-7207. ISSN 0888-5885

Fakatselis, T.E. (2002). Residence time optimization in continuous crystallizers. *Crystal Growth and Design*, Vol.2, No.5, (September 2002), pp. 375-379, ISSN 1528-7483

Feng, L. & Berglund, K. A. (2002). ATR-FTIR for determining optimal cooling curves for batch crystallization of succinic acid. *Crystal Growth and Design*, Vol.2, No.5, (September 2002), pp. 449-452, ISSN 1528-7483

Févotte, G. & Klein, J. P. (1995). Crystallization calorimetry for the assessment of batch seeding and cooling police. *The Chemical Engineering Journal,* Vol.59, No.2, (October 1995), pp.143-152, ISSN 1385-8947

Fujiwara, M.; Nagy, Z. K.; Chew, J. W. & Braatz, R. D. (2005). First-principles and direct design approaches for the control of pharmaceutical crystallization. *Journal of Process Control,* Vol.15, No.5, (August 2005), pp. 493-504, ISSN 0959-1524

Gahn, C. & Mersmann, A. (1995). The brittleness of substances crystallized in industrial-processes. *Powder Technology*, Vol.85, No.1, (October 1995), pp. 71-81, ISSN 0032-5910

Gaiao, EN.; Martins, VL.; Lyra, WS.; Almeida, LFA.; Silva, ECS. & Araújo, MCU. (2006). Digital image-based titrations. *Analytical Chimica Acta.* Vol.570, No.2, (Juno 2006), pp. 283-290, ISSN 0003-2670.

Gesthuisen, R.; Krämer, S.; Niggemann, G.; Leiza, J. R.; & Asua, J. M. (2005). Determining the best reaction calorimetry technique: theoretical development. *Computers and Chemical Engineering,* Vol.29, No.2,(January 2005) pp. 349-365 ISSN 0098-1354.

Giulietti, M.; Seckler, M. M.; Derenzo, S.; Ré, M. I. & Cekinski, E. (2001). Industrial crystallization and precipitation from solutions: State of the technique. *Brazilian Journal of Chemical Engineering*, Vol.18, No.4, pp. 423-440, ISSN 0104-6632

Gunawan, R.; Ma, D.L.; Fujiwara, M. & Braatz, R.D. (2002). Identification of kinetics parameters in multidimensional crystallization processes. *International Journal of Modern Physics B*, Vol.16, Nos.1-2, (January 2002), pp. 367-374, ISSN 0217-9792

Hernández, JA.; Heyd, B. & Trystram, G. (2008). On-line assessment of brightness and surface kinetics during coffee roasting. *Journal of Food Engineering.* Vol.87, No.3, (August 2008), pp. 314-322, ISSN 0260-8774.

Jolling, K.; Vandeven, M.; Eynden, JVD.; Amellot, M. & Kerkhove, EV. (2007). A highly reliable and budget-friendly Peltier-cooled camera for biological fluorescence imaging microscopy. *Journal of Microscopy.* Vol.228, No.3, (December 2007), pp. 264-271, ISSN 0022-2720.

Joung, O. J.; Kim, Y. H. & Fukui, K. (2005). Determination of metastable zone width in cooling crystallization with a quartz crystal sensor. *Sensors and Actuators B: Chemical*, Vol.105, No. 2, (March 2005), pp. 464-472, ISSN 0924-4005.

Kadam, S. S.; Mesbah, A.; der Windt, E. V. & Kramer, H. J. M. (2011). Rapid online calibration for ATR-FTIR spectroscopy during batch crystallization of ammonium sulphate in a semi-industrial scale crystallizer. *Chemical Engineering Research and Design*, Vol.89, No.7, (July 2011), pp. 995-1005, ISSN0263-8762.

Kail, N.; Briesen, H.; & Marquardt, W. (2008). Analysis of FBRM measurement by means of a 3D optical model. *Powder Technology* Vol.185 No.3 (July 2008) pp. 211-222, ISSN 0032-5910.

Kougoulos, E.; Jones, A. G.; Jennings, K. H.; & Wood-Kaczmar, M. W. (2005). Use of focused beam reflectance measurement (FBRM) and process video imaging (PVI) in a modified mixed suspension mixed removal (MSMPR) cooling crystallizer. *Journal of Crystal* Growth, Vol.273, Nos.3-4, (January 2005), pp. 529-534, ISSN 0022-0248

Lavanchy, F.; Fortini, S. & Meyer, T. (2004). Reaction calorimetry as a new tool for supercritical fluids. *Organic Process Research and Development,* Vol.8, No.3, pp. 504-510, ISSN 1083-6160.

Lewiner, F.; Klein, J.P.; Puel, F. & Fevotte, G. (2001). On-line ATR FTIR measurement of supersaturation during solution crystallization processes. Calibration and applications on three solute/solvent systems. *Chemical Engineering Science*, Vol.56, No.6, (March 2001), pp. 2069-2084, ISSN 0009-2509

Liang, RQ.; Tan, CY. & Ruan, KC. (2004). Colorimetric detection of protein microarrays based on nanogold probe coupled with silver enhancement. *Journal of Immunological Methods*, (February 2004), Vol.285, No.2, pp. 154-163, ISSN 0022-1759.

Liotta, V. & Sabesan, V. (2004). Monitoring and feedback control of supersaturation using ATR-FTIR to produce an active pharmaceutical ingredient of a desired crystal size. *Organic Process Research and Development*, Vol.8, No. 3, (May 2004), pp. 488-494, ISSN 1083-6160

Lyra, WS.; dos Santos, VB.; Dionízio, AGG.; Martins, VL.; Almeida, LF.; Gaião, EN.; Diniz, PHGD.; Silva, EC. & Araújo, MCU. (2009) Digital image-based flame emission spectrometry. *Talanta.* Vol.77, No.5, (May 2011), pp. 1584-1589, ISSN 0039-9140.

Ma, D. L.; Chung, S.H.; Braatz, R. D. (1999). Worst-case performance analysis of optimal batch control trajectories. *Aiche Journal*, Vol.45, No.7, (July 1999), pp. 1469-1486, ISSN 0001-1541

Maleki, N.; Safavi, A. & Sedaghatpour, F. (2004). Single-step calibration, prediction and real samples data acquisition for artificial neural network using a CCD camera. *Talanta*. Vol.64, No.4, (November 2004), pp. 830-835, ISSN 0039-9140.

Marciniak, B. (2002). Density and ultrasonic velocity of undersaturated and supersaturated solutions of fluoranthene in trichloroethylene, and study of their metastable zone width. *Journal of Crystal Growth,* Vol.236, No.1-3, (March 2002), pp. 347-356, ISSN 0022-0248

Marisol, IW.; Bijou, B. & Von Stockar, U. (1985). Use of a novel heat-flux calorimeter for the measurement of heat generated during growth of *K. fragilis* on lactose. *Thermochimica Acta* Vol.85, No.93, (April 1985), pp. 497-500, ISSN 0040-6031.

Man, Y. B. C.; Syahariza, Z. A. & Rohman, A., Fourier Transform Infrared (FTIR) Spectroscopy: Development, Techniques and Application in the Analyses of Fats and Oils, editor Oliver J. Rees, Nova Science Publishers, Inc. (2010).

Mantelis, CA. & Meyer, T. (2008). Supercritical reaction calorimetry: Versatile tool for measuring heat transfer properties and monitoring chemical reactions in supercritical fluids. *Industrial and Engineering Chemistry Research*, (May 2008), Vol.47, No.10, pp. 3372-3379, ISSN 0888-5885.

Mersmann, A. (2001) *Crystallization Technology Handbook.* Marcel Dekker Inc., New York.

Mullin, J. W. (2001). *Crystallization.* (4thed), Butterwoth-Heinemann, ISBN 075064833.3, Oxford, UK.

Nguyen, TNP. & Kim, KJ. (2008). Kinetic study on hemipenta hydrate risedronate monosodium in batch crystallization by cooling mode Original. *International Journal of Pharmaceutics*, (November 2008), Vol.364, No.1, pp. 1-8, ISSN 0378-5173.

Nýlvt, J.; Hostomsky, J. & Giulietti, M. (2001). *Cristalização.* IPT/UFSCar, ISBN85-85173-63-7, São Paulo, Brazil.

Paulaime, A. M.; Seyssiecq, I. & Veesler, S. (2003). The influence of organic additives on the crystallization and agglomeration of gibbsite. *Powder Technology*, Vol.130, Nos.1-3, (February 2003), pp. 345-351, ISSN 0032-5910

Perlberg, A.; Lorenz, H. & Seidel-Morgenstern, A. (2005). Crystal growth kinetics via isothermal seeded batch crystallization: Evaluation of measurement techniques and application to mandelic acid in water. *Industrial and Engineering Chemistry Research*, Vol.44, No. 4, (February 2005), pp. 1012-1020, ISSN 0888-5885

Podder, J. (2002). The study of impurities effect on the growth and nucleation kinetics of potassium dihydrogen phosphate. *Journal of Crystal Growth*, Vol.237-239 Part 1, (April 2002), pp. 70-75, ISSN 0022-0248.

Pöllänen, K.; Häkkinen, A.; Reinikainen, S. P.; Louhi-Kultanen, M.; & Nyström, L. (2006). A Study on Batch Cooling Crystallization of Sulphathiazole: Process Monitoring Using ATR-FTIR and Product Characterization by Automated Image Analysis. *Chemical Engineering Research and Design,* Vol.84, (January 2006), No.1, pp. 47-59, ISSN 0263-8762.

Qu, H.; Alatalo, H.; Hatakka, H.; Kohonen, J.; Louhi-Kultanen, M.; Reinikainen, S. P.; & Kallas, J. (2009). Raman and ATR FTIR spectroscopy in reactive crystallization: Simultaneous monitoring of solute concentration and polymorphic state of the crystals. *Journal of Crystal Growth* Vol.311, (June 2009), No.13, pp.3466-3475, ISSN 0022-0248

Rauls, M.; Bastosch, K.; Kind, M.; Kuch, St.; Lacmann, R. & Mersmann, A. (2000). The influence of impurities on crystallization kinetics – a case study on ammonium sulfate. *Journal of Crystal Growth*, Vol.213, Nos.1-2, (May 2002), pp.116-128, ISSN 0022-0248.

Safavi, A.; Maleki, N.; Rostamzadeh, A. & Maesum, S. (2007). CCD camera full range pH sensor array. *Talanta.* Vol.71, No.1, (January 2007), pp. 498-501, ISSN 0039-9140.

Seiceira, R.; Higa, CM.; Barreto, AG. & da Silva, JFC. (2005). Determination of kinetic parameters and Hammett ρ from the synthesis of triaryl phosphites using reaction calorimetry. *Thermochimica Acta* Vol.428, No.1-2, pp. 101-104, ISSN 0040-6031.

Sheikhzadeh, M.; Trifkovic, M.; & Rohani, M. (2008). Real-time optimal control of an anti-solvent isothermal semi-batch crystallization process. *Chemical Engineering Science.* Vol.63, (February 2008), No.3, pp.829-839, ISSN 0009-2509.

Shirshov, YM.; Khoruzhenko, VY.; Kostyukevych, KV.; Khristosenko, RV.; Samoylova, IA.; Pavlunchenko, AS.; Samoylov, AV. & Ushenin, YV. Analysis of some alcohols molecules based on the change of RGB components of interferentially colored calixarene films. *Sensors Actuators B: Chemical*. Vol.112, pp. 427-436, ISSN 0925-4005.

Silva, J.F.C. & Silva, A.P.M. (2011). Determination of the Adipic Acid Solubility Curve in Acetone by Using ATR-FTIR and Heat Flow Calorimetry. *Organic Process Research and Development*. Vol.15, No.4, (May 2011), pp. 893-897, ISSN 1083-6160.

Simon, LL.; Nagy, ZK. & Hungerbuhler, K. (2009). Endoscopy-based in situ bulk video imaging of batch crystallization processes. *Organic Process Research and Development,* Vol.13, No.6, pp. 1254-1261, ISSN 1083-6160.

Sun, Y.; Song, X.; Wang, J.; Luo, Y. & Yu, J. (2010). Determination of seeded supersolubility of lithium carbonate using FBRM. *Journal of Crystal Growth,* Vol.312, No.2, (January 2010) pp. 294-300, ISSN 0022-0248.

Teychené, S.; Autret, J. M. & Biscans, B. (2004). Crystallization of efflucimibe drug in a solvent mixture: effects of process conditions on polymorphism. *Crystal Growth and Design*, Vol.4, No.5, (September 2004), pp. 971-977, ISSN 1528-7483

Ulrich, J. & Strege, C. (2002). Some aspects of the importance of metastable zone width and nucleation in industrial crystallizers. *Journal of Crystal Growth*, Vol.237-239 Part 3, (April 2002), pp. 2130-2135, ISSN 0022-0248

Yu, Z. Q.; Tan, R. B. H. & Chow, P. S. (2005). Effects of operating conditions on agglomeration and habit of paracetamol crystals in anti-solvent crystallization. *Journal of Crystal Growth*, Vol.279, No.3-4, (June 2005), pp. 477-488, ISSN 0022-0248

Yu, L. X.; Lionberger, R. A.; Raw, A. S.; D'Costa, R.; Wu, H. & Hussain, A. S. (2004). Applications of process analytical technology to crystallization processes. *Advanced Drug Delivery Reviews*, Vol.56, No. 3, (February 2004), pp. 349-369, ISSN 0169-409X